

2019

A Comparative Study of Al and Bi Addition in the Transparent Conductive ZnO Thin Films Prepared by Spray Ultrasonic Method

F. Chouikh

Laboratory of Materials : Elaborations-Properties-Applications, Jijel University, Jijel 18000, Algeria,
fethichouikh@yahoo.fr

Y. Beggah

Laboratory of Materials : Elaborations-Properties-Applications, Jijel University, Jijel 18000, Algeria,
fethichouikh@yahoo.fr

N. Ariche

Laboratory of Materials : Elaborations-Properties-Applications, Jijel University, Jijel 18000, Algeria,
fethichouikh@yahoo.fr

M. Biréme

Laboratory of Materials : Elaborations-Properties-Applications, Jijel University, Jijel 18000, Algeria,
fethichouikh@yahoo.fr

G. Leroy

Unité de dynamique et structure des matériaux moléculaire, Université du Littoral Côte d'Opale 62228 Calais, France, fethichouikh@yahoo.fr

Follow this and additional works at: <https://digitalcommons.aaru.edu.ao/ijfst>

See next page for additional authors

Recommended Citation

Chouikh, F.; Beggah, Y.; Ariche, N.; Biréme, M.; Leroy, G.; and Waldhoff, N. (2019) "A Comparative Study of Al and Bi Addition in the Transparent Conductive ZnO Thin Films Prepared by Spray Ultrasonic Method," *International Journal of Thin Film Science and Technology*. Vol. 8 : Iss. 3 , Article 2.
Available at: <https://digitalcommons.aaru.edu.ao/ijfst/vol8/iss3/2>

This Article is brought to you for free and open access by Arab Journals Platform. It has been accepted for inclusion in International Journal of Thin Film Science and Technology by an authorized editor. The journal is hosted on [Digital Commons](#), an Elsevier platform. For more information, please contact rakan@aaruo.edu.ao, marah@aaruo.edu.ao, u.murad@aaruo.edu.ao.

A Comparative Study of Al and Bi Addition in the Transparent Conductive ZnO Thin Films Prepared by Spray Ultrasonic Method

Authors

F. Chouikh, Y. Beggah, N. Ariche, M. Biréme, G. Leroy, and N. Waldhoff

A Comparative Study of Al and Bi Addition in the Transparent Conductive ZnO Thin Films Prepared by Spray Ultrasonic Method

F. Chouikh^{1*}, Y. Beggah¹, N. Ariche¹, M. Biréme¹, G. Leroy², N. Waldhoff² and M. S. Aida^{3,4}

¹ Laboratory of Materials : Elaborations-Properties-Applications, Jijel University, Jijel 18000, Algeria

² Unité de dynamique et structure des matériaux moléculaire, Université du Littoral Côte d'Opale 62228 Calais, France

³ Department of Physics, Faculty of Sciences, King Abdulaziz University, 21589 Jeddah, Saudi Arabia

⁴ Center of Nanotechnology, King Abdulaziz University, Jeddah, Saudi Arabia

Received: 13 May. 2019, Revised: 7 Aug. 2019, Accepted: 10 Aug. 2019

Published online: 1 Sep. 2019

Abstract: Zinc oxide (ZnO) is a binary semiconductor material with direct band gap (3,3 eV) because of their good optoelectronics properties. ZnO thin films find several applications such as: solar cells, gas sensors, piezoelectric sensors, waves guides. ZnO thin films can be prepared by several techniques: spray parolysis, thermal evaporation, reactive sputtering, sol gel, laser ablation.

In this present work and in order to obtain conducting transparent layers, ZnO thin films were deposited by ultrasonic spray technique on glass and silicon substrates. The investigate is focused on the doping level influence of the structural, optical and electrical properties of ZnO thin films. Two dopants were used Bismuth and Aluminium. In the starting solution Bismuth and Aluminium where used with a variation of the doping rate from 0 to 5 % mol .

X-ray diffraction patterns confirm that all films are crystalline and the preferred orientation depends on the dopant nature and concentration.

The optical characterization of deposited films was carried out using UV-Vis spectrometry in the spectral range 200-800 nm. The analysis of the transmittance spectra allows us to deduce the film thicknesses optical band gaps, and Urbach energy. Hence, the values of the gap were found to be between 3.19 to 3.31 eV.

The electrical measurements were made using the two points technique. From the results, we concluded that the electrical conductivity of doped ZnO layers is higher than that of undoped layers and the effect of Bismuth was more pronounced on the evolution of the conductivity than Aluminium.

Keywords: ZnO, thin films, ultrasonic spray, transmission, Urbach energy, XRD.

1 Introduction

Transparent conductive oxide (TCO) layer is crucial and important in the fabrication of thin film solar cells in order to transmit the sunlight to the absorber layer. The TCO layer in solar cell should be well optimized so that it has high transparency as well as low electrical resistivity. ZnO [1,2], InSnO [3] and SnO₂ [4]. are some common materials to be widely used as window layer in solar cell? Among the TCOs [5], ZnO, Zinc oxide is one of the most

important multifunctional materials with direct band gap of 3.37 eV and exciton binding energy up to 60 meV giving rises to efficient excitonic emission at room temperature even somewhat above [6]. Besides, due to the high chemical stability, the high transmittance, the low deposition temperature, the non-toxic, the high material availability and Zn is abundant element. [7,8].

Intrinsic and doped ZnO materials are used as laser diodes [9], solar cells [10,11], sensors [12], piezoelectric devices [11], catalysts for liquid phase hydrogenation [13], transparent electrodes [14], surface acoustic wave (SAW), and acoustic-optic devices [15].

*Corresponding author: fethichouikh@yahoo.fr

ZnO thin films have been deposited by many techniques such as sputtering [16], chemical vapour deposition [17], sol-gel [18], laser ablation [19] and spray pyrolysis, either pneumatic [20] or ultrasonic [21,22]. The last technique has been widely used, because it is simple, more reproducible, without toxicity, and cost effective as it does not require sophisticated vacuum apparatus. Moreover, incorporation of dopants is easier by this technique. [23] The effect of different dopants such as Al [24-27], In [25, 28], Fe [29], Ga [30], Er [31] and others, on the properties of ZnO thin films has been investigated.

2 Experimental Details

All the thin films samples were deposited by (USP) technique. The schematic representation of the spray system has been described in previous work [32]. The pure ZnO film was prepared by dissolving an appropriate amount of zinc acetate dehydrate ($\text{Zn}(\text{CH}_3\text{COO})_2 \cdot 2\text{H}_2\text{O}$) with 0.02 M concentration in methanol solution (CH_3OH). Doping of Al and Bi at (1 to 5 wt.%) were achieved by adding aluminum chloride (AZO films) and Bismuth nitrate (BZO films), respectively in the starting solution. The glass and silicon substrates were used and cleaned thoroughly with Acetone, The Methanol and finally with deionized water with the help of an ultrasonic bath. The structural properties of the films were studied by X-Ray Diffraction (XRD), using Cu-ka radiation of wavelength $\lambda = 0.15418$ nm. The size of the crystallites was calculated from the Scherer's formula [33]. The thickness was determined from ellipsometric measurements performed on ZnO films deposited onto the Si substrates. The transmittance of the layers deposited on glass was measured in the UV-Visible region using the Shimadzu

3101PC double beam spectrophotometer. The gap energy E_g of the ZnO films, deposited on glass substrates, was determined from Tauc formula [34]. The absorption coefficient α ($\alpha h\nu$), in the spectral region of the light's absorption, was deduced from the Beer-Lambert law [35]. The Urbach tail was determined from the variation of $\log(\alpha)$ with the incident photon energy $h\nu$ [36]. The electrical properties of the layers were determined using the I(V) characteristics by the two probes technique in a coplanar structure with two evaporated gold electrodes.

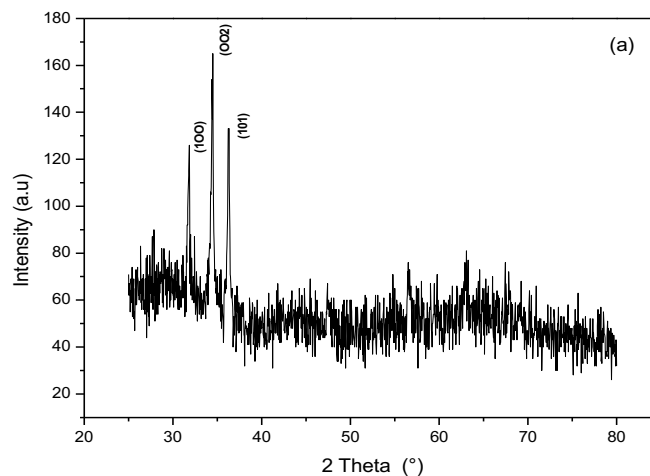
3 Structural Analysis

The XRD data were used to investigate the structural properties after incorporation of Bi and Al atoms in the ZnO thin films. Fig 1 shows X-ray diffractograms of pure ZnO (a), ZnO:Bi (b) and ZnO:Al (c) thin films, deposited at 350°C by spray pyrolysis. This analysis reveals that all the films are polycrystalline and composed of wurtzite-type ZnO phase without any impurity phase.

The X-ray patterns for undoped ZnO show three main peaks corresponding to (100), (002) and (101) planes of the ZnO wurtzite phase. These random orientations are conforming to the fact that crystallites grew randomly on glass substrate.

A switching in the growth orientation of the crystallites from the random orientation to (100) plane is observed when Bi atoms are added (Fig 1c). This change in the growing orientation is related to the films nucleation process.

The ZnO:Al films Unlike ZnO:Bi films show a preferential orientation in the (002) direction along c-axis perpendicular to the substrate surface plane (Fig 1b). This result is generally observed in ZnO thin films, regardless the deposition techniques since this plane (002) requires less energy to be formed.



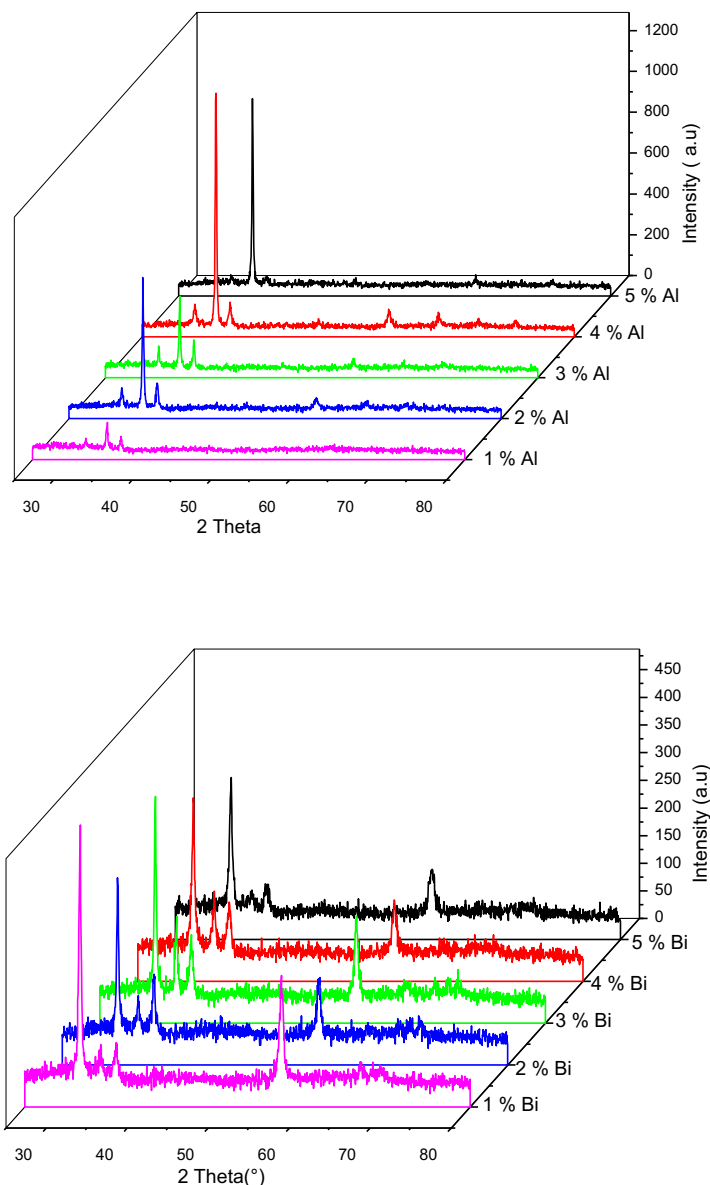


Fig. 1: X-ray diffractograms for (a) ZnO (b) ZnO:Bi and (c) ZnO:Al.

3.1 Texture

The texture coefficient is calculated to describe the preferential orientation using the following formula [37]:

$$TC_{(hkl)} = I_{(hkl)} / [I_{(100)} + I_{(002)} + I_{(101)}]$$

As can be seen in Fig. 2, it is clear that orientation of ZnO thin films is influenced by the nature and the concentration of doping atoms. The texture coefficient TC (100) of ZnO:Bi films (Fig 2.A) increases sharply with adding 1% of Bi doping and decreases gradually with further increase in the doping concentration, but the direction (100) remains

the preferential orientation. Jiang et al. [38] obtained the same results with a less intense peak. We should also note that this change in the preferential orientation is also reported in Indium doped Zinc oxide IZO thin films deposited by spray pyrolysis by Goyal et al. [39]. They have observed a change from (002) as preferential orientation to (101) with In doping and to (100) with increasing doping level.

In the case of ZnO:Al films, the texture coefficient TC (002) increases with increasing Al concentration (Fig 2.B). This indicates that Al doping leads to an improvement of the crystalline quality of the films.

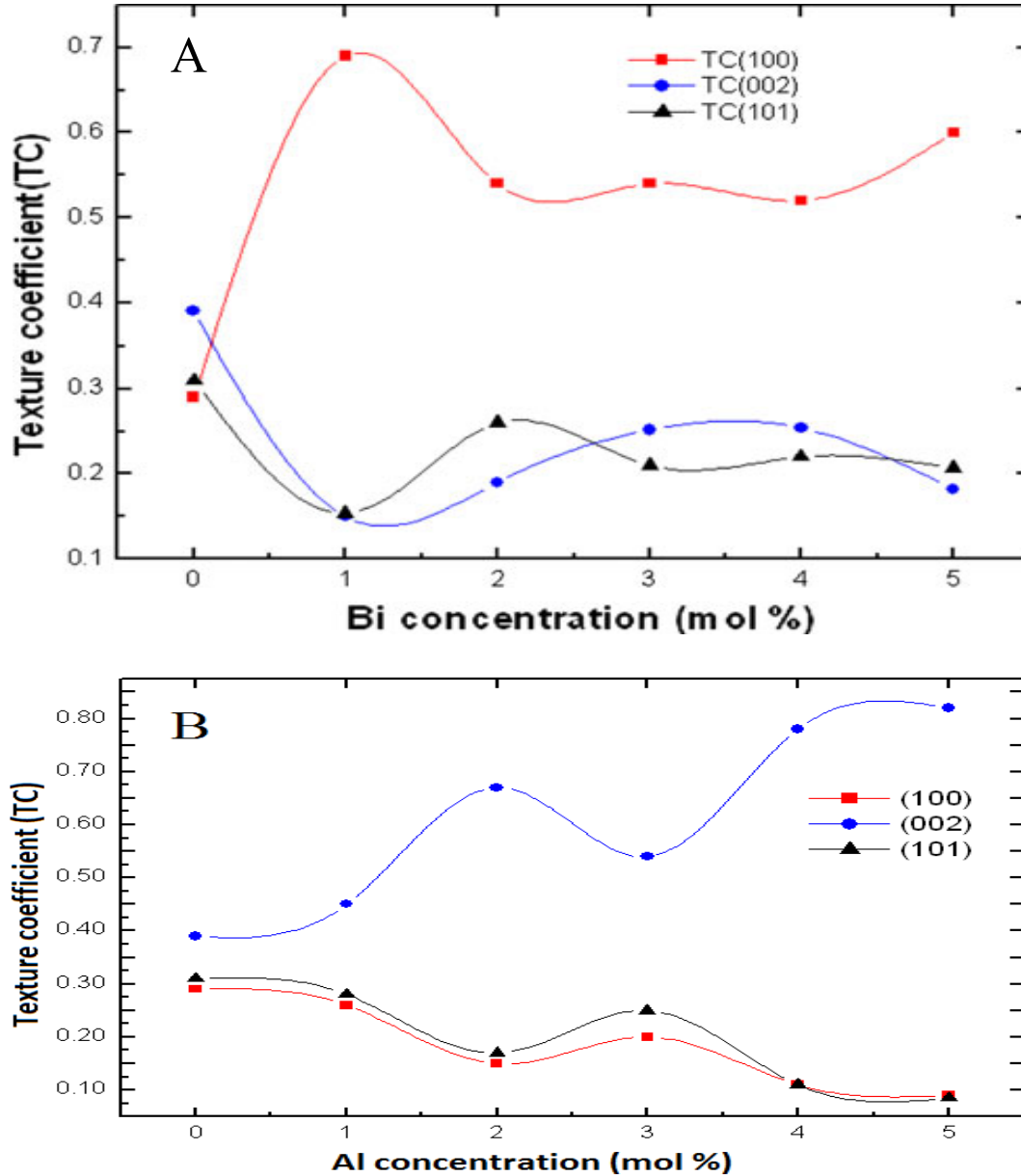


Fig.2: Variation of the texture coefficient TC (100), TC (002) and TC (101) of ZnO films with (A) Bi and (B) Al concentrations.

3.2 Grains Size

The grains size of different samples was determined using the XRD spectra and the Debye-Scherrer formula [33]:

$$D = \frac{K}{\beta \cdot \cos\theta_{hkl}} \lambda$$

Where λ is the X-ray wavelength (0.15418 nm), θ is the Bragg angle expressed in radians, and β is the full width at

half-maximum (FWHM) of the most intense peak ((100) for ZnO:Bi and (002) for ZnO:Al), K equal to 0,9 is the constant which depends on the shape of the crystallite.

The variation of the grain size for ZnO:Bi and ZnO:Al thin films with Bi and Al concentration, , are respectively shown in Fig. 3.

The grain size increases sharply at low doping level. It varies from 19 nm with undoped film to 83 nm with 1% Bi doped ZnO, however, with further increasing in doping level, the grain size decreases. This evolution can be interpreted in terms of disorder create in the crystal lattice by the incorporation of the Bi ions. Despite the fact that Bi atoms incorporation preserve the hexagonal wurtzite

structure, which proves that our layers are still stable. The Bi atoms incorporation in the film network may alter the nucleation step during film growth; the presence of Bi ions reduces the nucleation centres which consequently reduce the grain size of the crystallites. The same conclusion was reported by Kumar et al. [41] in In doped ZnO thin films, Srinivasan et al. [42] in Mn doped ZnO and Paul et al. [43] in Zr Doped ZnO thin films. In ZnO:Al thin films, as the concentration of Al increases, we observe an increase in the crystallites size. This result agrees with the increase of the intensity of the diffraction peaks and thus the highly textured films at high concentrations. Furthermore, this result assures the incorporation of Al atoms in the ZnO lattice. The parameters of the (002) diffraction peak of different samples are summarized in the table.1 below:

3.4 Stress

The stresses in our films were estimated from the observed shift, in the diffraction peak, between their position in recorded XRD spectra and in ASTM cards and by using the formula of Hoffmann [44].

$$\sigma = \left[2C_{13} \frac{(C_{11} + C_{12})C_{33}^{Couche}}{C_{13}} \right] e_{zz}$$

Where $C_{33}^{Couche} = \frac{0.99C_{33}^{Cristal}}{1 - e_{zz}}$ and $e_{zz} = \frac{c_0 - c}{c_0}$.
 C_{ij} are the elastic constants of ZnO

given by the following values [45]:
 $C_{11} = 209.7$ GPa, $C_{12} = 121.1$ GPa, $C_{13} = 105.1$ GPa and $C_{33} = 210.9$ GPa.

The results obtained are represented in Fig. 4. The origin of the stress in undoped ZnO thin films is due to the deposition technique and the temperature of the substrate. However, in the case of the ZnO:Bi, it is due to the incorporation of Bi atoms in the film network. As seen in Fig. 4, at low concentration, the stress increases with the rate of doping, in this case the stress is induced by the size of Bismuth atoms which is bigger compared to Zn size. On the other hand, this increase in the stress suggests that the Bi atoms occupy the substitutional sites at low doping level. However, from 1% doping level the stress is relaxed. The stress relaxation with the increasing in the doping level can be related to the inter-gain segregation of Bi dopant atoms at large doping level. Choi et al. [46] has reported, in Ga doped ZnO thin films by RF magnetron, that excess of Ga atoms, above a certain critical concentration in ZnO thin films, segregates into the grain boundaries. This segregation alters the electrical conductivity of doped films because the dopant will be electrically inactive (cf 5 Electrical Characterizations).

For ZnO:Al thin films, it is observed that the stress decreases to a minimum value then increases in the larger values of the Al quantity. This evolution can be explained as follow: Al atoms with ionic radius smaller than that of Zn may occupy substitutional sites at low doping rate. At high concentration, we suggest that substitutional sites are saturated and thus Al atoms are forced to occupy interstitial sites leading to the increase of stress.

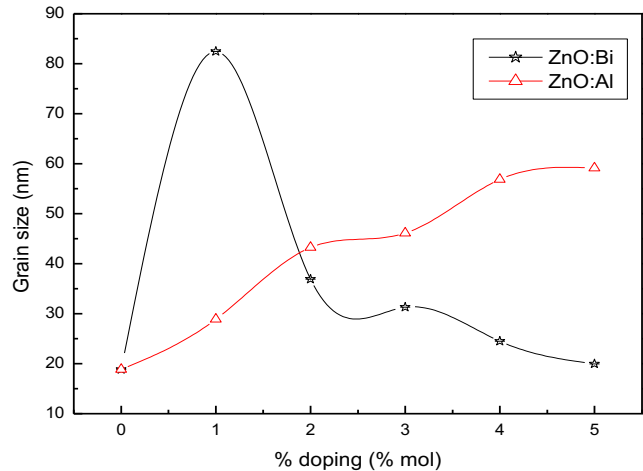


Fig. 3: Variation of the crystallite size of ZnO: Bi and ZnO: Al thin films deposited by spray pyrolysis with doping concentration.

Table 1: Parameters of the (002) diffraction peak of ZnO, ZnO:Bi and ZnO:Al thin films at various concentration of Bi and Al

Samples		2 Thêta (°) (002)	$d_{hkl}(A^\circ)(002)$	$C_{maille}(A^\circ)$
Pur ZnO		34.423	2.605	5.21
ZnO:Bi	1% Bi	34.407	2.607	5.214
	2% Bi	34.373	2.609	5.218
	3% Bi	34.417	2.606	5.212
	4% Bi	34.451	2.603	5.206
	5% Bi	34.466	2.602	5.204
ZnO:Al	1% Al	34.468	2.602	5.204
	2% Al	34.410	2.606	5.212
	3% Al	34.437	2.604	5.208
	4% Al	34.399	2.607	5.214
	5% Al	34.401	2.607	5.214

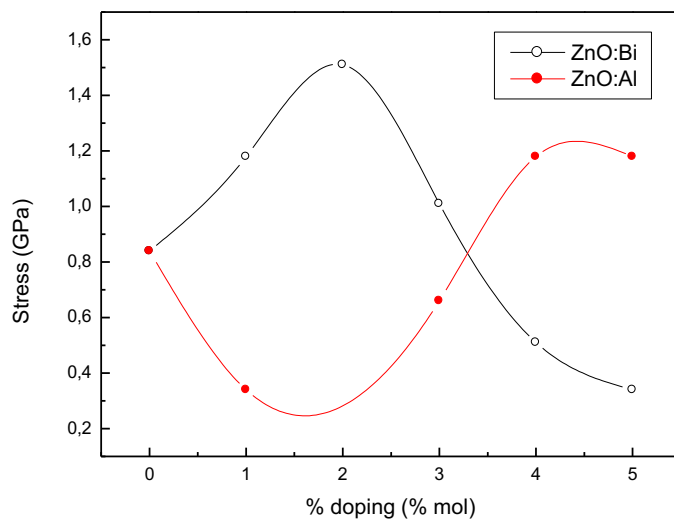


Fig .4: Stress of ZnO: Bi and ZnO: Al thin films deposited by spray pyrolysis.

4 - UV-VIS STUDY

4.1 Transmittance

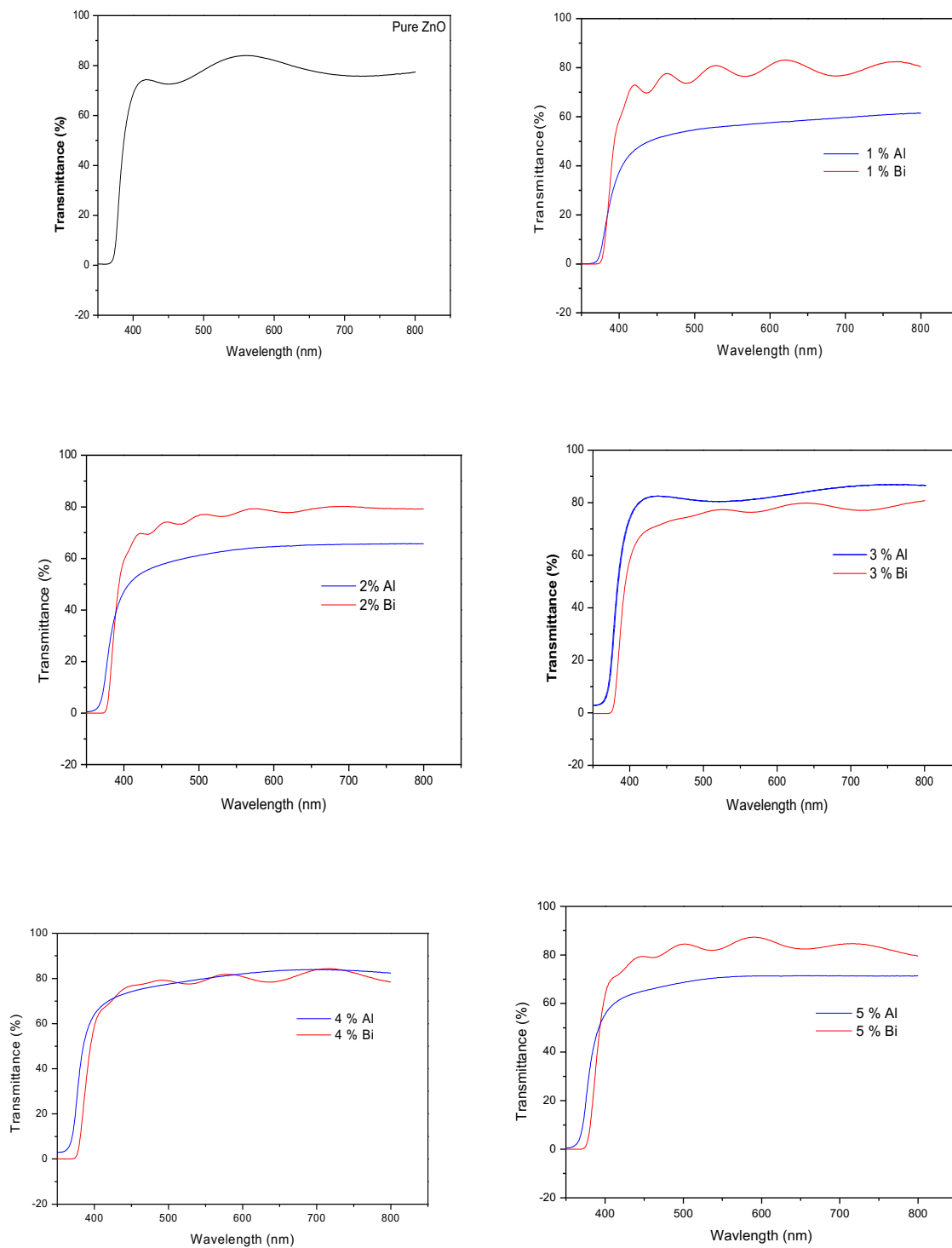


Fig. 5: Optical transmission spectra of ZBO and ZAO films.

In Fig 5 we have reported the UV-VIS optical transmission spectra of ZnO, ZBO and ZAO thin films deposited with spray technique. The obtained films are highly transparent in the visible range, with an excellent transmission (>80%).

4-2 Optical Gap

For ZBO thin films, the interference fringes observed in the spectrum indicates, that the deposited films are homogeneous with a smooth surface. A sharp cut-off between 367 and 406.64 nm is also observed. In the other hand, the films transmittance was not affected by Bi incorporation with different concentration. The same feature was observed by Lee et al. [47] in Al doped ZnO thin films from 1 to 5% deposited by spray pyrolysis.

For ZAO thin films, the presence of the interference fringes in spectra is due to the multiple reflections at the interface's films/substrate and film/air. The presence of the fringes translates that our films are sufficiently thick and the smooth light scattering at the film surface and enhances the light transmission.

All the films exhibit an abrupt absorption edge below 400 nm, this is due to the onset of the fundamental absorption of ZnO. From these spectra, one can infer that the doping (Al) concentration slightly affects the transmittance of the films.

In Fig 6, we have reported the variation of the optical gap of doped ZnO thin films. The optical gap was estimated from the well-known linear extrapolation of the variation of $(\alpha h\nu)^2$ as a function of the incident photon energy $h\nu$, where α is the absorption coefficient calculated from the transmission spectra (calculated as $(1/d) \ln (1/T)$; d : film thickness, and T : optical transmittance) and $h\nu$ is the photon energy. This estimation procedure is widely used for direct transition semiconductors, which obeys the following relation [48]:

$$(\alpha h\nu)^2 \sim (h\nu - E_g).$$

For ZBO thin films, it is noticed that the value of E_g increases from 3.19 to 3.24 eV with doping, this widening of the gap according to the Moss–Burstein theory [49, 50], in heavily doped zinc oxide films; shows that the donor electrons occupy states at the bottom of the conduction band. Since the Pauli principle prevents states from being doubly occupied and optical transitions are vertical, the Valence electrons require an additional energy to be excited to higher energy states in the Conduction band. Therefore, E_g of doped zinc oxide is broader than undoped zinc oxide films, this phenomenon has been also mentioned by Lee et al. [51].

With low concentration of the doping agent Al, the value of E_g increases from 3.19 eV to 3.31 eV. The gap reduction in the 4%-5 % interval is the result of the occupation of the interstitial sites by the Al doping atoms, because the latter, represent the principal native donors in the ZnO films [52]. The interpretation of the variation of the gap with the Al doping levels corroborates well with the statement in the last section, where it is mentioned that with 3 % of doping ratio, Al atoms occupy the interstitial sites in the matrix of

Zinc oxide. This is appropriate with the interpretation of the reduction in transmittance to strong percentage of Aluminium.

4.3 Urbach Energy

We note that the values of the gap recorded in the case of Al are higher than those recorded for Bi.

The calculated Urbach energy in Bi doped ZnO films varies from 11 to 530 meV. These results are comparable with the work already made by Bourguine et al. [35]. It is worth noting that the Urbach energy is related to the disorder in the film network. Therefore, the increase in the latter (Fig.7) with Bi doping is due to the induced distortion in the material network since Bi atoms has a larger size than Zn atoms.

In the other hand, the calculated Urbach energy in our films varies from 78 to 170 meV.

Given the minimal value of low dopant concentration reaffirms the stability of the films and the increase of Urbach energy with the doping ratio is very logical and also ensures the incorporation of Al atoms in ZnO matrix, this increase is found by B.N.Pawar et al [52], and interpreted by the donor levels of interstitial zinc atoms [53].

5- Electrical Characterization

In this last part, the resistivity of undoped (ZnO) and doped Zinc oxide (ZBO and ZAO) was investigated .

Electrical measurements were done after giving electrical contacts using Gold target in the form of two end contacts having distance about 1 cm between them.

The undoped ZnO sample has a resistivity of $1,9 \cdot 10^2 \Omega \cdot \text{cm}$. The electrical properties of Bi and Al doped ZnO thin films have been drastically improved in comparison with undoped ZnO thin films

Figures 8 shows the variation of electrical resistivity with the various percentages of Bi and Al doping in the ZBO and ZAO thin films deposited by spray pyrolysis. At 2 % Bi and Al doping, the film has lowest resistivity of $0.11 \cdot 10^{-2} \Omega \cdot \text{cm}$.

It is clearly observed that the resistivity variation with concentration doping is the same in both cases, ZBO and ZAO films.

The decrease in resistivity with different dopant concentrations is attributed to the replacement of Zn^{2+} by Bi^{3+} and Al^{3+} ions which introduce a large number of electrons in the doped films. Thus, the conductivity of the film increases. However, a further increase in Bi and Al doping to above 2 % raises the resistivity. Indeed at a higher doping concentration of above 2 %, the disorder produced in the lattice (due to the difference in the ionic radius of Zn^{2+} , Bi^{3+} and Al^{3+} increases the efficiency of scattering mechanism such as phonon scattering and ionized impurity scattering which, in turn, causes an increase in resistivity [54]. The other reason is the

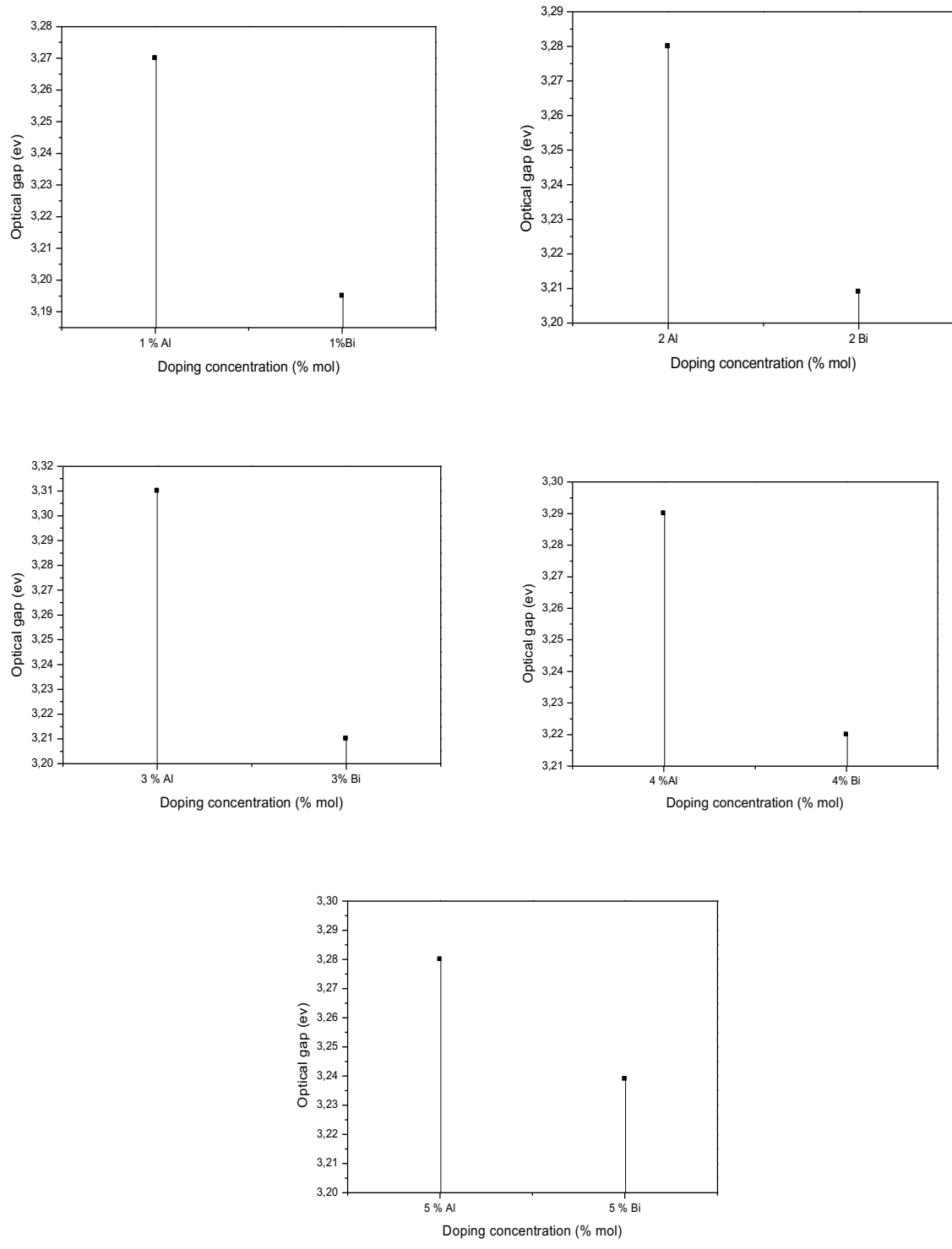


Fig. 6 : Variation of direct band gap with Bismuth and Aluminium content in the films .

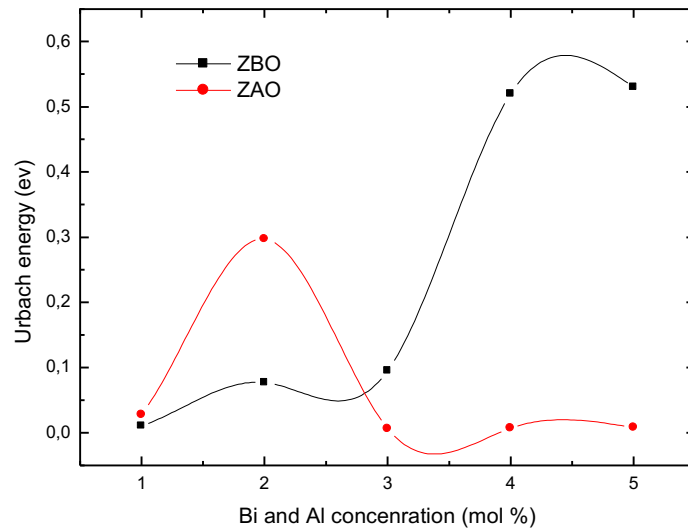


Fig.7: Evolution of Urbach energy of ZBO and ZAO films with Bi and Al concentrations.

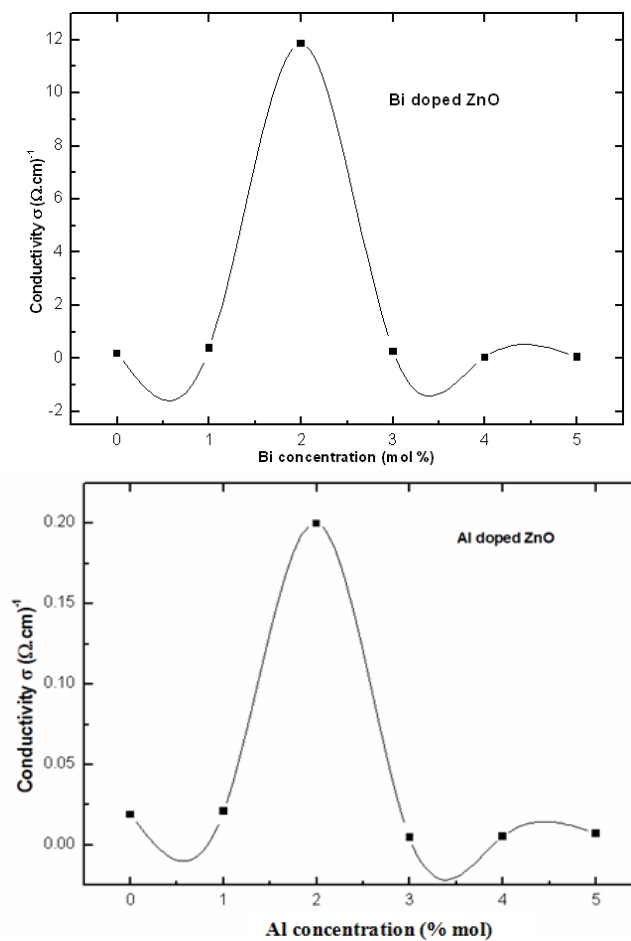


Fig. 8: Evolution of dark room conductivity of ZBO and ZAO films with Bi and Al concentrations.

segregation of neutral Bi and Al atoms at the grain boundaries, in heavily doped samples, which do not contribute free electrons [55]. The same behaviour of the reduction in the dark conductivity after a critical doping level is reported by many authors with different doping atoms [56, 57].

It has been found, that this is due to the preparation technique and experimental conditions. In the present study, we observed that 2 % is the optimum value of Bi and Al in ZnO to obtain good electrical properties.

6 Conclusions

In the present work and in order to obtain conducting transparent layers, the ZnO thin films were deposited by ultrasonic spray technique on glass and silicon substrates. Our interest is focused on the investigation of the doping level influence on the structural, optical and electrical properties of ZnO thin films. Two dopants Bismuth and Aluminium were varied the rate of doping from 0 to 5% mol in the starting solution.

X-ray diffraction patterns confirm that all films are crystalline and the preferred orientation depends on the nature and concentration dopant.

The optical characterization of deposited films was carried out using UV-Vis spectrometry in the spectral range 200-800 nm. The analysis of the transmittance spectra allows us to deduce the films thicknesses optical band gaps, and Urbach energy. Hence, the values of the gap were found to be between 3.19 to 3.31 eV.

The electrical measurements were made using the technique of two points. From the results, we concluded that the electrical conductivity of doped ZnO layers is higher than that of undoped layers and the effect of Bismuth was more pronounced on the evolution of the conductivity than Aluminium.

From our experiments we have demonstrated that the physical properties of ZnO can be well modified by Bi and Al doping, and the optical and electrical properties of the new ZBO films are better than the classical ZAO layers.

References

[1] M.A. Martinez, J. Herrero, M.T. Gutierrez, Deposition of transparent and conductive Al-doped ZnO thin films for photovoltaic solar cells, *Solar Energy Materials and Solar Cells.*, **45**, 75–86, 1997.

[2] B. Rech, S. Wider, C. Beneking, A. Loffi, O. Kluth, W. Reetz, H. Wagner, Proc. Of the 26th IEEE Photovoltaic Specialists Conference, Anaheim., 619, 1997.

[3] L. Davis, Properties of transparent conducting oxides deposited at room temperature, *Thin Solid Films.*, **236** 1–5, 1993.

[4] H. Schade, Z.E. Smith, Optical properties and quantum efficiency of a-Si_{1-x}C_xB:H/a-SiB:H solar cells, *Journal of Applied Physics.*, **57**, 568–574, 1985.

[5] M.L. Cohen, J.R. Chelikowsky, *Electronic Structure and Optical Properties of Semiconductors*, 2nd ed., Springer-Verlag, Berlin., 81, 1989.

[6] S. Tuzemen, E. Gur, Principal issues in producing new ultraviolet light emitters based on transparent semiconductor zinc oxide, *Opt. Mater.*, **30**, 292, 2007.

[7] B.H. Kim, J.H. An, Highly c-axis oriented ZnO film on silica glass using zinc

[8] H. Wang, M.H. Xu, J.W. Xu, L. Yang, S.G. Zhou, Effects of annealing temperature and thickness on microstructure and properties of sol-gel derived multilayer Al-doped ZnO films, *J. Mater. Sci.*, **21**, 145, 2010.

[9] C. Liu, J.A. Zapien, Y. Yao, X. Meng, C.S. Lee, S. Fan, Y. Lifshitz, S.T. Lee, *Adv. Mater.*, **15**, 838–841, 2003.

[10] Z.S. Wang, C.H. Huang, Y.Y. Huang, Y.J. Hou, P.H. Xie, B.W. Zhang, H.M. Cheng, *Chem. Mater.*, **13** 678–682, 2001.

[11] K. Westermark, H. Rensmo, T.A.C. Lees, J.G. Vos, H.T. Siegbahn, *J. Phys. Chem. B.*, **106**, 10108–10113, 2002.

[12] H.M. Lin, S.J. Tzeng, P.J. Hsiau, W.L. Tsai, *Nanostruct. Mater.*, **10**, 465–468, 1998.

[13] G.M. Hamminga, G. Mul, J.A. Moulijn, *Chem. Eng. Sci.*, **59**, 5479–5485, 2004.

[14] S. Jager, B. Szyszka, J. Szczyrbowski, G. Brauer, *Surf. Coat. Technol.*, **98**, 1304, 1998.

[15] Y. Yoshino, T. Makino, Y. Katayama, T. Hata, *Vacuum.*, **59**, 538, 2000.

[16] C.A.O. Yongee, Lei Miao, Sakae Tanemura, Masaki Tanemura, Yohei Kuno, Yasuhiko Hahashi, Yukimasa Mori, *Jpn. J. Appl. Phys.*, **45**, 1623–1628, 2006.

[17] T.A. Polley, W.B. Carter, D.B. Poker, *Thin Solid Films.*, **357**, 132–136, 1999.

[18] B. Kotlyarchuk, V. Savnuck, M. Oszwaldowski, *Cryst. Res. Technol.*, **40**, 1118–1123, 2005.

[19] Susan Huang, Tatiana Kaydanova, Alex Miedaner, David S. Ginley, U.S. Dept. Energy *J. Undergraduate Res.*, **4**, 70–73, 2004.

[20] C.E. Benouis, A. Sanchez Juarez, M.S. Aida, *J. Appl. Sci.*, **7(2)**, 220–225, 2007.

[21] C.E. Benouis, M. Benhaliliba, A. Sanchez Juarez, M.S. Aida, F. Chami, F. Yakuphanoglu, *J. Alloys Compd.*, **490**, 62–67, 2010.

[22] M. Benhaliliba, C.E. Benouis, A. Sanchez Juarez, M.S. Aida, F. Chami, F.

[23] F. Paraguay, D.J. Morales, W. Estrada, L.E. Andrade, M. Miki-Yoshida, *Thin Solid Films.*, 366, 16–27, 2000.

[24] M.A. Kaid, A. Ashour, *Appl. Surf. Sci.*, **253**, 3029–3033, 2007.

[25] A. Chakrabortya, T. Mondal, S.K. Bera, S.K. Sen, R. Ghosh, G.K. Paul, *Mater. Chem. Phys.*, **112**, 162–166 2008.

[26] B. Joseph, P.K. Manoj, V.K. Vaidyan, *Ceram. Int.*, **32**, 487–493, 2006.

[27] J.-H. Lee, B.-O. Park, *Mater. Sci. Eng.*, **B 106**, 242–245, 2004.

- [28] M.A. Lucio-Lopez, M.A. Luna-Arias, A. Maldonado, M. de la L. Olvera, D.R. Acosta, *Solar Energy Mater. Solar Cells.*, **90**, 733–741, 2006.
- [29] U. Alver, T. Kılınc, E. Bacaksız, S. Nezir, *Mater. Sci. Eng.*, **B 138**, 74–77, 2007.
- [30] M. de L. Olvera, A. Maldonado, *Phys. Status Solidi A* **196**, 410, 2003,
- [31] M. Alaoui Lamrani, M. Addou, Z. Sofiani, B. Sahraoui, J. Ebothe, A. El Hichou, N. Fellahi, J.C. Bernede, R. Dounia, *Optics Commun.*, **277**, 196–201 2007.
- [32] F. Chouikh . Y. Beggah . M. S. Aida .*J Mater Sci: Mater Electron* DOI 10.1007/s10854-010-0167-y., **22**,499, 2011.
- [33]. P. Scherrers, *Gott. Nachr.*, **2**, 98, 1918.
- [34] J.J. Tauc, *Amorphous and Liquid Semiconductor* (Plenum, New York, 1976)
- [35] A. Bougrine, A. El Hichou, M. Addou, J. Ebothe', A. Kachouna, M. Troyon, *Mater. Chem. Phys.*, **80**, 438–445, 2003.
- [36] M.V. Kurik, *Phys. Status solidi (a)* 8–9, 1971.
- [37] X. Jiwei, Z. Liangying, Y. Xi, *Ceram.Lnt.*, **26**, 883 2000.
- [38] M. Jiang, X. Liu, *J. Mater. Sci.: Mater. Electron.*, **20**, 972–976, 2009.
- [39] D.J. Goyal, C. Agashe, M.G. Takwale, V.G. Bhide, *J. Mater. Res*, **8**, 1052, 1993.
- [41] P.M. Kumar, C.S. Kartha, P. Vijayakumar, *J. Appl. Phys.*, **98**, 023509, 2005.
- [42] G. Srinivasan, J. Kumar, *Cryst. Growth* (2007)
- [43] G.K. Paul, S. Bandyopadhyay, *Mater. Chem. Phys.*, **79**, 71, 2003.
- [44] K.T. Ramakrishna Reddy, T.B.S. Reddy, I. Forbes, R.W. Miles, *Surf. Coat. Technol.*, 151–152, 110–113 2002.
- [45] T.B. Bateman, *Appl. Phys.*, **33(11)**, 3309, 1962.
- [46] B. Choi, H.B. Im, *Thin Solid Films.*, **712**, 193-194, 1990.
- [47] J.H. Lee, B.O. Park, *Mater. Sci. Eng.*, **B106**, 242–245, 2004.
- [48] P. Sreedhara Reddy, et al., *Solid State Commun.*, **12** 899, 1991.
- [49] T.S. Moss, *Proc. Phys. Soc. Lond.*, **B 67**, 775, 1954.
- [50] B.E. Sernelius, K.F. Berggren, Z.C. Jin, I. Hamberg, C.G. Granqvist, *Phys. Rev.* **B 37**, 17, 1988.
- [51] K.E. Lee, M. Wang, E.J. Kim, S.H. Hahn, *Curr. Appl. Phys.*, **9**, 683–687, 2009.
- [52] B.N. Pawar, S.R. Jadkar, M.G. Takwal. *Solar Energy Materials & solar cell.*
- [53] J. Song, I-Jun Park and Kyung-Hoon Yoon, *Journal of the Korean Physical Society.*, 219-224, 1996.
- [54] B. Joseph, P.K. Manoj, V.K. Vaidyan, *Ceram. Int.*, **32** 487–493, 2006.
- [55] P.K. Nayak, J. Yang, J. Kim, S. Chung, J. Jeong, C. Lee, Y. Hong, *J. Phys. D: Appl. Phys.*, **42**, 035102, 2009.
- [56] T. Prasada Rao, M.C. Santhosh Kumar, A. Safarullaa, V. Ganesan, S.R. Barman, C. Sanjeeviraja, *Physica.*, **B** **405**, 2226–2231, 2010.
- [57] K.T. Ramakrishna Reddy, T.B.S. Reddy, I. Forbes, R.W. Miles, *Surf. Coat. Technol.*, 151–152, 110–113, 2002.